Metal-one-dimensional Peierls semiconductor interface phenomena

1993 J. Phys.: Condens. Matter 5 4631

(http://iopscience.iop.org/0953-8984/5/27/008)

J. Phys.: Condens. Matter 5 (1993) 4631–4640. Printed in the UK

Metal–one-dimensional Peierls semiconductor interface phenomena

M E Itkis†, F Ya Nad'†, P Monceau‡ and M Renard‡

† Institute of Radioengineering and Electronics, Russian Academy of Sciences, Mokhovaya 11, 103907 Moscow, Russia

‡ Centre de Recherches sur les Très Basses Températures, BP 166, 38042 Grenoble Cédex 9, France

Received 24 November 1992, in final form 26 March 1993

Abstract. The spatial distribution of the electric field E between two current terminals along the quasi-one-dimensional TaS_3 conductor has been studied using a multicontact configuration. In the low-temperature range ($30 < T < 50$ K) for a DC voltage V applied between current terminals less than the threshold value V_T, we have measured a strong increase of E near the negative terminal with respect to its value in the middle of the sample. In contrast, E is reduced near the positive terminal. The distribution of E revealed by these experiments is supposed to be related to the formation of two Schottky barriers on the metal–Peierls semiconductor contacts which are biased one in the reverse and the other in the forward direction. The region of increased E corresponds to the depletion layer near the negative terminal. When V is increased, both the size of this region L and the appropriate band bending in the Peierls semiconductor are enlarged. In the range $V > V_T$ the spatial distribution of E is governed by an additional voltage developed near both current terminals to maintain the conversion of the current of electrons in the sliding charge-density-wave condensate. In this case the electric field increases near both contacts and the spatial distribution of E becomes more symmetrical.

1. Introduction

Under the influence of various forces such as electric field, pressure, thermal gradients, etc, the charge-density waves (CDW) in quasi-one-dimensional (Q1D) conductors develop elastic and plastic deformations (see [1,2] and references therein). As a result, variations in conductivity and in optical properties, hysteretic effects, shift of the narrow band frequency in the sliding state, etc have been observed.

In a number of works, it was shown that the CDW deformation in Q1D conductors between two current terminals is non-uniform. Measurements of the remanent CDW deformation after the application of current pulses of magnitude larger than the threshold current I_T show that the CDW is stretched near one terminal and compressed near another terminal [3,4]. These deformations cause local variations of conductivity with opposite signs.

The spatial distribution of the remanent CDW deformation was measured by means of laser beam scanning [5]. It was shown that the electrical conductivity variation due to the CDW deformation is caused by the shift of the chemical potential of quasi-particles (electrons and holes) which is needed to neutralize the variation of the local charge density induced by the deformed CDW [5,6]. Similar results were obtained by measuring the remanent CDW deformation with a mobile contact [7]. With the same technique of mobile contact the spatial distribution of the potential $V(x)$ along the sample length has also been measured with non-zero applied current [8,9]. In orthorhombic TaS_3 at $T = 120$ K an additional voltage δV

0953-8984/93/274631+10$07.50

was shown to develop, which has approximately identical amplitude near both terminals ($\Delta V/V \simeq 5\%$). At $T = 78$ K the distribution of $\delta V(x)$ becomes asymmetrical. At the negative terminal, the $\delta V/V$ value reaches 10% and δV exceeds the Δ/e value, where Δ is the energy gap, while at the positive contact the voltage growth is considerably smaller. The interpretation of these results was based on the concept of the shift of the chemical potential level due to CDW deformations. However, in this context, it was impossible to explain the large δV value ($\delta V > \Delta/e$) and the difference in δV values near both terminals.

In the present work, using a multicontact configuration, we have measured the spatial distribution of the electric field, $\boldsymbol{E}$, between the two current terminals in the sliding CDW mode of QID conductors. This distribution, which depends on the magnitude and the direction of the applied current, has been studied in the low-temperature range between 30 and 120 K. We have determined the characteristic size of the region of non-uniform electric field near terminals as a function of the current and of the temperature. We give a qualitative explanation of these results taking into account both the effects of the metal–Peierls semiconductor interface and the specific features of the CDW motion for E above the threshold field E_T.

2. Experiment

We have investigated the spatial distribution of electric field $\boldsymbol{E}$ along the orthorhombic TaS_3 samples with typical sizes $10 \times 1 \times 2000\ \mu m^3$. The scheme of the multicontact measurements is shown in figure 1. The 16 gold or platinum strips evaporated on a sapphire substrate were used as electrical contacts. These strips were 8 μm wide and separated by variable distances, between 40 μm and 200 μm. The TaS_3 sample was placed across the strips. The 16 electrical contacts between the strips and the sample were established due to electrostatic attraction of the TaS_3 sample and the dielectric substrate. This method of contact preparation was developed earlier for $NbSe_3$ samples [10].

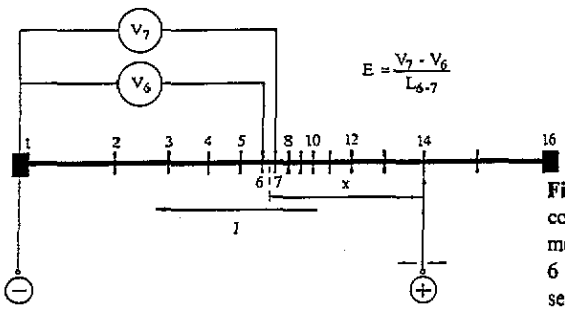

Figure 1. Scheme of the experiment. 1–16 are the contact strips. V_6 and V_7 are two electrometers for measuring the potential difference between probes 6 and 7. x is the distance between the centre of segment 6–7 and the movable current contact.

As it can be seen from figure 1 two electrometers were used to measure the potential difference between two potential probes 7 and 6. The electric field E averaged over the small distance $L_{6-7} = 40$ μm was obtained as $E = (V_7 - V_6)/L_{6-7}$. The distance L_{6-7} is much smaller than the length of the whole sample $L_{1-16} \simeq 2000$ μm, so this field E may be considered as a local field $E(x)$ characterizing the small part of the sample. Firstly the current was injected through the ends of the sample (contacts 16 and 1). The $E(x)$ distribution at fixed current was determined by successively switching the positive contact from position 16 towards position 8 (figure 1), which is equivalent to moving our small

segment 6–7 towards the positive current contact. After every switching the local electric field E as a function of a distance x from the positive current contact was measured. The negative current contact was fixed at position 1 far enough from the segment 6–7 ($L_{1-6} \simeq 800$ μm) that it did not disturb the field in this segment. The $E(x)$ distribution near the negative current contact was obtained with the same procedure but reversing the polarity of the current contacts. To avoid the scattering of data due to the dependence of the properties of the CDW on temperature and electric field prehistory [11, 12], we have performed the $E(x)$ measurements beginning with the large current $I \gg I_T$ and then decreasing the current.

The typical value of contact resistance R_C obtained at room temperature was ~ 1 kΩ. At low temperatures, $T < 100$ K, R_C increased, roughly proportional to the resistance of the whole volume. This behaviour is typical for the processes of current spreading near a small-area contact. Using the transformation from the anisotropic to isotropic case we can estimate the spreading resistance at low temperatures $T < 100$ K. This estimation shows that for the majority of the contacts the effective contact area is about 50% of the total geometrical contact area (sometimes it is about 10%), which is probably due to the roughness of contact surfaces and absorbed atoms. It can be shown that the potential contacts may be considered as unperturbative with fulfilment of the inequality $R_C/R_V \gg 1$, where R_V is the resistance of part of the sample with a length approximately equal to twice the length of the contact strip. This inequality is satisfied in the whole temperature range investigated.

As it will be shown below an unusual $E(x)$ distribution develops within the sample when the same contacts are used for current injection. The investigation of this phenomenon is the subject of our work. In spite of some scattering of the contact resistance values, the results obtained did not depend on the individual properties of the contacts.

3. Results

We have carried out a detailed study of the spatial distribution of electric field $E(x)$ between two current contacts as a function of temperature and current. The results obtained from different batches were similar. Below we show the results for three samples under investigation. The majority of our measurements have been performed on the insufficiently known region of low temperatures below ~ 60 K. Figures 2(a) and 3(a) show the spatial $E(x)$ distribution in sample A2 ($T = 48.6$ K) and B7 ($T = 35.5$ K) and its variation with the applied current. Figure 2(b) shows the conductivity σ normalized to the value at room temperature as a function of the mean electric field $\bar{E} = V_{1-16}/L_{1-16}$ for sample A2. The curves of the $E(x)$ distribution labelled 1–8 in figure 2(a) were obtained for the values of the mean electric field $\bar{E}$, which are indicated by the same figures for the $\sigma(\bar{E})$ dependence (figure 2(b)). The region of ohmic conductivity ($\bar{E} < E_T'$), the region of weak non-linearity with threshold electric field E_T' and the region of strong non-linearity with threshold field E_T are distinguished in the $\sigma(E)$ dependence [13, 14]. The $\sigma(\bar{E})$ dependences for samples B7 and A2 are qualitatively similar.

As can be seen from figures 2(a) and 3(a) for a weak electric field $E \simeq E_T'$ a certain non-uniformity of E has already developed (curves 1 on both figures). With increasing mean electric field $\bar{E}$ in the region between E_T' and E_T the non-uniformity of the electric field near the contacts grows and it spreads out along a long distance from the contacts (figures 2(a) and 3(a), curves 4). In this region the $E(x)$ distribution has an asymmetrical form: a large growth of electric field when approaching the negative contact and a decrease of electric field but with a smaller amplitude near the positive one.

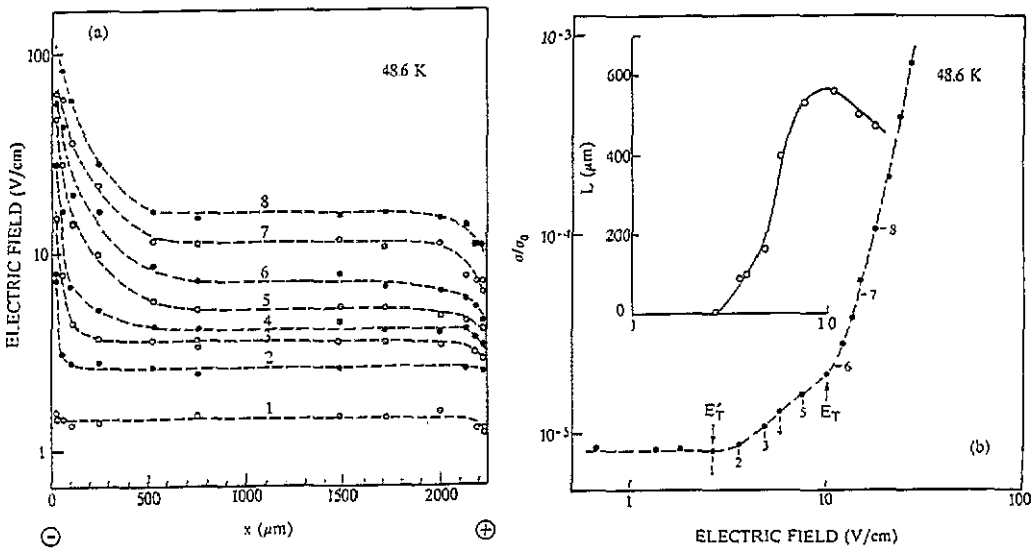

Figure 2. (*a*) Spatial distribution of electric field $E(x)$ in sample A2 ($T = 48.6$ K) at fixed currents. Current magnitudes for curves are 1, 1×10^{-9} A; 2, 2×10^{-9} A; 3, 4×10^{-9} A; 4, 6×10^{-9} A; 5, 1×10^{-8} A; 6, 2×10^{-8} A; 7, 5×10^{-8} A; and 8, 1×10^{-7} A. (*b*) Conductivity σ normalized to its room-temperature value σ_0 as a function of mean electric field $\bar{E}$ for sample A2. The figures near the $\sigma(\bar{E})$ curve correspond to the same currents as in (*a*). The inset shows the length L corresponding to the region of non-uniformity of $E(x)$ near the negative current contact as a function of the mean electric field.

It is convenient to describe the magnitude of the non-uniformity and the asymmetry of the $E(x)$ distribution by the ratio $\Delta E/E_0$, where E_0 is the electric field in the middle of the sample and ΔE is equal to the difference between the electric field E_M measured at the shortest distance near the current contact and E_0: $\Delta E = E_M - E_0$. Figure 3(*c*) shows the $\Delta E/E_0$ dependences for the negative contact (open circles) and for the positive contact (filled circles). As can be seen from figure 3(*c*), the $\Delta E/E_0$ values have different signs at opposite-polarity contacts. Their amplitudes grow with increasing $\bar{E}$ and they reach extrema at $\bar{E} = E_T$ (the maximum for the negative contact and the minimum for the positive one). The $E(x)$ distribution becomes most asymmetrical near $\bar{E} \simeq E_T$ (figure 3(*a*), curves 5 and 6). For $\bar{E} > E_T$ the $\Delta E/E_0$ value near the negative contact begins to decrease (figure 3(*c*)). $\Delta E/E_0$ near the positive contact also decreases with increasing $\bar{E}$ above E_T, goes through zero and changes its sign. In this electric field range the form of the $E(x)$ distribution corresponds to the growth of the local electric field near both contacts (figure 3(*a*), curve 9 and figure 3(*c*)). For a higher electric field, $\bar{E} \gg E_T$, the $E(x)$ distribution becomes more and more symmetrical (figure 3(*a*), curve 10).

The length L on which the non-uniformity of the electric field spreads out from the contacts within the sample is one of the most important quantities that are derived by this effect. In this work we determine L as the distance between the current contact and a point in the sample where magnitude ΔE increases by 10% with respect to the electric field E_0 in the middle of the sample. With another determination of L, for example as the distance for which the magnitude ΔE is two times smaller than its value E_M near the contacts, the dependences of L on temperature and electric field have a qualitatively similar form. The $L(E)$ dependences for the negative contact are shown in figures 2(*b*) and 3(*b*) for samples

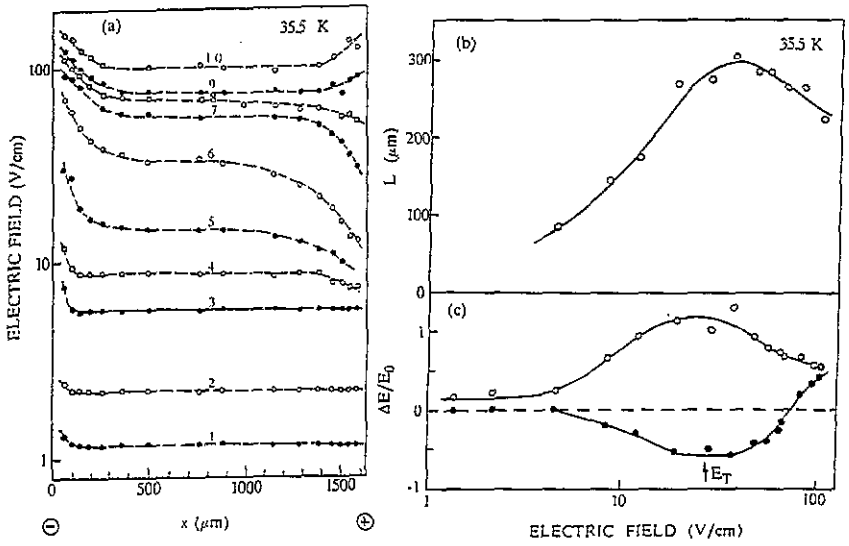

Figure 3. (*a*) Spatial distribution of local electric field $E(x)$ in sample B7 ($T = 35.5$ K) at fixed currents. Current magnitudes for curves are 1, 1×10^{-10} A; 2, 1.6×10^{-10} A; 3, 4×10^{-10} A, 4, 7×10^{-10} A; 5, 1.5×10^{-9} A; 6, 4×10^{-9} A; 7, 1.5×10^{-8} A; 8, 5×10^{-8} A; 9, 1.5×10^{-7} A; and 10, 1×10^{-6} A. (*b*) Length L corresponding to the region of non-uniformity of $E(x)$ near the negative contact, as a function of the mean electric field. (*c*) Relative magnitude of the non-uniformity $\Delta E/E_0$ as a function of the mean electric field for negative contact (open circles) and positive contact (filled circles). E_0 is the electric field in the middle of the sample.

A2 and B7, respectively. The growth of L begins for $\bar{E}$ below E_T and continues up to E_T. Near $\bar{E} = E_T$ the L value approaches a maximum. In this electric field range the non-uniformity of the $E(x)$ distribution spreads out for a long distance of ~ 500 μm for the A2 sample and ~ 300 μm for the B7 sample. At $E > E_T$ some decrease of the magnitude of L is observed.

In the high-temperature range ($T > 100$ K) the character of the $E(x)$ distribution is considerably changed. Figure 4 shows the $E(x)$ distribution for different current levels at $T = 117$ K. The development of non-uniformity near the contacts and the growth of L begin at $E > E_T$ (curve 2). Increasing electric field is observed near both contacts, i.e. the $E(x)$ distribution is symmetrical at high temperatures in accordance with [5] and [9]. With increasing temperature the relative amplitude of non-uniformity $\Delta E/E_0$ decreases.

We have compared the $L(T)$ values of different samples obtained at the fields $\bar{E}(T)$ that correspond to an equal relative development of the non-linearity in the $\sigma(E, T)$ dependences. Figure 5 shows the dependence of L on the reciprocal of temperature $L(T)$ obtained for such $\bar{E}$ magnitudes when the conductivity σ is ten times higher than the ohmic conductivity. As can be seen, when T is decreased, the L value grows approximately by one order of magnitude and at $T < 50$–60 K, L tends to saturation at the level of several hundreds of microns. Using another evaluation for the $L(T)$ dependence, when L is determined for $\bar{E} = 3E_T$, the $L(T)$ dependence is qualitatively similar.

4. Discussion

From the foregoing it follows that in Q1D CDW conductors a non-uniform distribution of

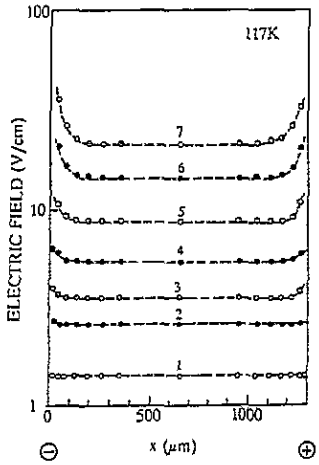

Figure 4. Spatial distribution of electric field $E(x)$ in sample B6 (T = 117 K) at fixed currents. Current magnitudes for curves are 1, 5×10^{-7} A; 2, 1.5×10^{-6} A; 3, 5×10^{-6} A; 4, 1.5×10^{-5} A; 5, 5×10^{-5} A; 6, 1.5×10^{-4} A; and 7, 3×10^{-4} A.

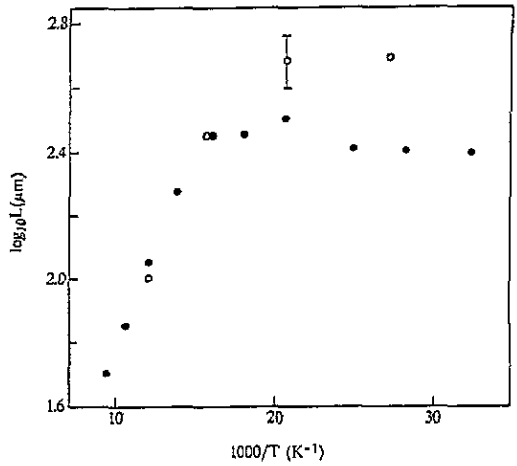

Figure 5. Variation of the length revealing the non-uniformity of $E(x)$ near the negative current constant as a function of reciprocal temperature for samples A2 (open circles) and B7 (filled circles). For each temperature the field $E(x)$ is such that the conductivity $\sigma(E)$ is ten times higher than the ohmic conductivity.

the electric field is observed, the character of which changes with current and temperature. This question has been considered in a number of theoretical works. However, we do not know a sufficiently complete theory which is adequate for explanation of the dependences observed. Perhaps this can be attributed to the complexity of this problem. For this reason we will only attempt to present below a qualitative explanation of the results obtained.

The most simple explanation of the spatial non-uniformity of electric field near current terminals could be the non-uniform current spreading near the small-area contact with the highly anisotropic Q1D conductor. The results obtained, which show that the contact resistance grows proportionally to the volume resistance, could favour this explanation. However, the contribution of the spreading resistance should be revealed as a symmetric growth of electric field near both current terminals. In our experiments a strongly asymmetric $E(x)$ distribution is observed which varies considerably as a function of the current amplitude and current direction. In addition, the estimation of the characteristic length of current spreading $l_s = d\sqrt{\sigma_\parallel/\sigma_\perp}$ (where d is the sample's thickness, and $\sigma_\parallel$ and $\sigma_\perp$ are the longitudinal and transverse conductivities respectively) shows that $l_s \simeq 10$ μm at 100 K and 50 μm at 30 K, which is considerably smaller than the characteristic length of the $E(x)$ distribution observed by us. Therefore, the effect of current spreading seems not to play an appreciable role in our measurements, and another explanation should be put forward.

We will make the assumption that at $T < T_P$ and for weak electric field, $E \ll E_T$, Q1D conductors are similar to semiconductors and that they show their specific properties due to CDW motion mainly in the high-electric-field range, $E > E_T$. This dual nature of these materials can be demonstrated with measurements performed at low temperatures when the free electron concentration is small. As can be seen from figure 2(*a*) (curve 1) at low temperatures and for weak electric field, $E \simeq E_T'$, a small non-uniformity already exists at $E \to 0$ but with a very small amplitude. Most probably such a distribution of E is due to the contact phenomena of the metal (Au, Pt)–Peierls semiconductor (TaS_3) interface

associated with the formation of Schottky barriers [15].

At low temperatures the CDW is a well developed three-dimensional superstructure—'electron body' [16] with energy gap Δ. In the ground state of this superstructure two main types of excitations can be developed: the first type is single-particle excitations (electrons and holes) due to thermal generation across the Peierls gap just as in semiconductors. The electrons and holes can contribute to both longitudinal $\sigma_\parallel$ and transverse $\sigma_\perp$ conductivities (naturally taking into account the anisotropy). The second type is collective excitations due to local CDW deformations near defects and impurities. These CDW excitations correspond to amplitude and phase solitons which have a charge, effective mass and which are capable of moving through the crystal as quasi-particles [17]. In particular, the phase solitons have the activation energy $\simeq T_P$, which is smaller than the Peierls gap, and they are capable of moving without dissociation only along the crystal chains, contributing solely to $\sigma_\parallel$.

In o-TaS_3 at temperatures between T_P and $\sim$ 100 K, $\sigma_\parallel$ and $\sigma_\perp$ show an activated decrease with the same activation energy $\Delta \simeq 800$ K, i.e. caused by thermally activated electrons and holes [13, 14]. Below 100 K the activated dependence of $\sigma_\perp$ keeps the same $\Delta \simeq 800$ K which indicates the conservation of the single-particle mechanism for the tranverse conductivity [13]. Simultaneously the $\log \sigma_\parallel(1/T)$ dependence deviates from linearity and evolves towards an average slope $\simeq T_P$. These results and a number of others published earlier [13, 14, 18, 19] show that at $T < 100$ K the contribution of collective excitations in $\sigma_\parallel$ begins to prevail.

When a Peierls semiconductor such as TaS_3 is put in an intimate contact with a metal the common chemical potential for quasi-particles must be established. This can be achieved by charge transfer from the semiconductor into the metal conduction band. However, the 'majority carriers' in the Peierls semiconductors, solitons and dislocations, are not able to cross the metal–semiconductor interface. However, near this interface and across the crystal these solitons can dissociate into free electrons [1], which are able to cross the metal–semiconductor interface. The negative charge transferred to the metal electrode must be screened by the positive space charge developed within the semiconductor. As a result the depletion layer and the appropriate band bending develop within the semiconductor with a potential barrier at the metal–semiconductor interface like a Schottky barrier [15]. In the case of usual semiconductors the space charge is generated by ionized impurities. In our opinion, for a Peierls conductor the space-charge and screening effects are determined by appropriate redistribution of solitons and dislocations taking into account their pinning and depinning at the impurity sites. In the stationary state near the metal electrode a potential well develops for solitons and dislocations [20]. We suppose that the observed non-uniformity of E near contacts at $E \simeq E'_T$ is due to the formation of a space-charge region and appropriate band bending within the Peierls semiconductor (figure 6(a)). In our experiments we have two current contacts and, as can be seen from figures 2(a) and 3(a) in the range $E < E_T$ near both contacts, the derivative dE/dx corresponds to the development of positive space-charge regions near the contacts.

For weak electric field, $E \simeq E'_T$, the non-uniformity of E and its characteristic size, L, are small (figure 2(a) and 3(a), curves 1). The considerable growth of non-uniform $E(x)$ distribution is correlated with the appearance of non-linear conductivity at $E > E'_T$ (figure 2(b)). As was shown earlier [13, 14] the non-linear conductivity at $E'_T < E < E_T$ can be ascribed to enhancement of the rate of depinning of the 'frozen-in' solitons and dislocations and to their transport which has a hopping character. This correlation is additional evidence in favour of connection of the space-charge origin with spatial redistribution of CDW collective excitations. With increasing E in the region $E'_T < E < E_T$ we observe the growth of both L (figures 2(b) and 3(b)) and the additional electric field

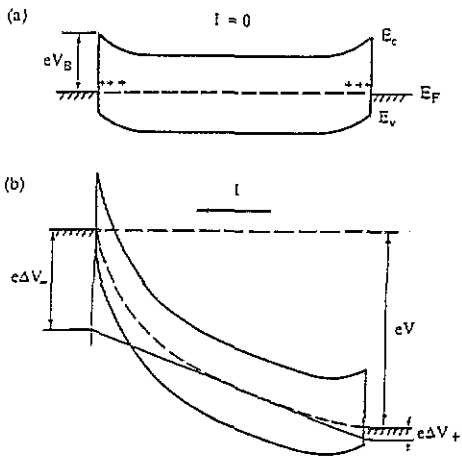

Figure 6. Energy diagram of two Schottky barriers developed at the metal–Peierls semiconductor contacts. (*a*) The current is equal to zero. eV_B is the potential barrier for electrons passing from the metal to semiconductor. E_c and E_v are the energy of the bottom of the conductivity band and the top of valence band, respectively. E_F is the Fermi level. (*b*) Non-zero current. V is the voltage across the sample. ΔV_- and ΔV_+ are additional voltages corresponding to band bending near the negative and positive contacts, respectively.

ΔE near contacts relative to the value E_0 in the middle of the sample (figure 3(*c*)). When E is increased the qualitative form of the $E(x)$ distribution is preserved: the increase of electric field near the negative contact and the decrease near the positive one. However both $\Delta E/E_0$ and L are quantitatively different for the two terminals. As a rule $\Delta E/E_0$ and L values near the negative contact are larger than those near the positive one (figures 2 and 3). We associate such an asymmetrical $E(x)$ distribution with the fact that the two current contacts are biased in the opposite way (figure 6(*b*)). The contact near the negative electrode is biased in the reverse direction [15]. Under this condition the band bending, the potential non-uniformity and the L value are larger near the negative electrode than near the positive one. The additional voltage near the negative electrode ΔV (figure 6(*b*)) can reach 600 mV which is considerably larger than the maximum possible shift of the chemical potential level within the CDW energy gap, $\Delta/e \simeq 60$ meV, developed due to the CDW deformation. It seems that the development of the large additional voltage near the negative electrode is mainly related to the band bending.

As was mentioned above, at low temperatures a large part of the conductivity is associated with the motion of solitons and dislocations. With increasing E the electron injection across the Schottky barrier grows. According to the theory [21] every two injected electrons turn into a 2π soliton near the contact. The solitons are added to the intrinsic solitons and dislocations which have been created under the influence of impurities and defects in the CDW superlattice. In our case the condition of injection at the negative contact which is biased in reverse direction and at the positive contact which is biased in forward direction are different. For example, electrons near the negative electrode undergo a higher electric field than near the positive one. As a result the processes of conversion of electrons to solitons can be different near these two contacts. These additional circumstances can make a contribution to the asymmetry of the $E(x)$ contribution. As one can see the processes involved here are rather complex and they cannot be reduced to similar processes to those in conventional semiconductors.

This difference becomes more evident when $\bar{E}$ approaches the threshold value E_T. In this region the conductivity grows abruptly, and narrow band noise and a number of other phenomena develop, which are attributed to the beginning of the CDW motion. The physical mechanism which provides the CDW motion is a phase slip in those parts of the sample where the phase gradient of the CDW deformed by the applied electric field exceeds some threshold value [2, 14, 22–25]. The solitons and dislocations created as a result of phase

slipping contribute to transport phenomena. At $E \simeq E_T$ a sharp change in CDW dynamics occurs. The CDW becomes more mobile. The concentration of solitons and dislocations grows and their screening effect greatly increases. Thus the growth of $\Delta E/E_0$ and L cease and they begin to decrease (figures 2(*b*), 3(*b*) and 3(*c*)).

Finally, at $E > E_T$ the processes of conversion of electron current into CDW current become dominant. As is known, an additional voltage is needed to maintain phase slipping [2, 10, 26, 27] and the motion of solitons, dislocations and dislocation lines which arise from soliton aggregation [21]. These processes mainly take place near current contacts, but they can spread out along a considerable distance within the sample [20, 21]. The fact that at $\bar{E} \simeq E_T$ the local electric field near the negative contact is higher than that near the positive one corresponds to experimental observations [28] where it has been shown that at $E > E_T$ the voltage pulses nucleate (as a result of phase slipping) first near the negative contact and then they propagate to the opposite contact. With subsequent growth of E the same processes gradually develop near the positive contact and the spatial $E(x)$ distribution becomes more and more symmetrical (figure 3(*a*) and 3(*c*)).

All the above-mentioned phenomena essentially reveal themselves in the low-temperature range. At higher temperatures ($T > 100$ K) on one hand the portion of electrons thermo-activated across the Schottky barrier increases, which reduces the influence of this barrier on the $E(x)$ distribution. On the other hand the volume concentration of thermo-activated electrons grows and consequently the screening length L is greatly reduced (figure 5). For these reasons, in the higher temperature range, in the weak field $\bar{E} < E_T$ the regions of the small $E(x)$ non-uniformities are practically invisible (figure 4, curve 1). At $\bar{E} > E_T$ the non-uniformity of the electric field becomes pronounced and the $E(x)$ distribution has a symmetrical form as in [9].

In conclusion, we demonstrate that in TaS_3 at low temperatures the electric field distribution is non-uniform and asymmetrical. The form of this distribution changes as a function of temperature and current. The data are interpreted on the basis of the suggestion that at low temperatures the dynamic properties of TaS_3 are determined by the motion of solitons and dislocations. The contact phenomena at the interface between the metal electrode and the Peierls semiconductor TaS_3 are shown to be the main reason for the asymmetry in the electric field distribuiton. The great magnitude of the additional voltage $\Delta V > \Delta/e$ developed near the contacts is accounted for by the band bending within the Peierls semiconductor.

Acknowledgments

We would like to acknowledge many useful discussions with S A Brazowskii and S I Matveenko. We thank F Levy for providing us with TaS_3 samples. One of the authors (MI) is very grateful to Centre de Recherches sur les Très Basses Températures, laboratoire associé à l'Université Joseph Fourier de Grenoble, for kind hospitality and to M E Gershenson for help in preparing the platinum strips on the substrate.

References

[1] Feinberg D and Friedel J 1989 *Low-Dimensional Electronic Properties of Molybdenum Bronzes and Oxides* ed C Schlenker (Dordrecht: Kluwer) p 407

[2] Nad' F 1989 *Charge Density Waves in Solids (Modern Problems in Condensed Matter Science 25)* ed L P Gor'kov and G Gruner (Amsterdam: Elsevier) p 191

[3] Janossy A, Mihaly G and Kriza G 1984 *Solid State Commun.* **51** 63
[4] Mihaly L and Janossy A 1984 *Phys. Rev.* B **30** 3530
[5] Itkis M E, Nad' F Ya and Pokrovskii V Ya 1986 *Sov. Phys.–JETP* **63** 177
[6] Artemenko S N, Volkov A F and Kruglov A N 1986 *Sov. Phys.–JETP* **64** 906
[7] Brown S E, Mihaly L and Gruner G 1986 *Solid State Commun.* **58** 177
[8] Zaitsev-Zotov S V 1987 *JETP Lett.* **46** 572
[9] Zaitsev-Zotov S V 1989 *Synth. Met.* **29** F433
[10] Monceau P, Renard M, Richard J and Saint-Lager M C 1986 *Physica* B **143** 318
[11] Higgs A W and Gill J C 1983 *Solid State Commun.* **47** 737
[12] Gill J C 1981 *Solid State Commun.* **39** 1203
[13] Zhilinskii S K, Itkis M E, Kalnova I Yu, Nad' F Ya and Preobrazhenskii V B 1983 *Sov. Phys.–JETP* **58** 211
[14] Itkis M E, Nad' F Ya and Monceau P 1990 *J. Phys.: Condens. Matter* **2** 8327
[15] Sze C M 1969 *Physics of Semiconductor Devices* (New York: Wiley)
[16] Anderson P W 1984 *Basic Notions of Condensed Matter Physics* (New York: Benjamin) chs 3, 4
[17] Brazovskii S A and Kirova N N 1984 *Soviet Scientific Reviews 1984 A: Physics Reviews* **6** ed I Khalatnikov (New York: Harwood) p 99
[18] Zhilinskii S K, Itkis M E and Nad' F Ya 1984 *Phys. Status Solidi* a **81** 367
[19] Biljaković K, Lasjaunias J C, Monceau P and Levy F 1989 *Europhys. Lett.* **8** 771
[20] Brazovskii S A and Matveenko S I 1992 *Sov. Phys.–JETP* **101** 1620
[21] Brazovskii S A and Matveenko S I 1991 *J. Physique* **1** 269, 1173
[22] Gor'kov L P 1983 *JETP Lett.* **38** 87; 1984 *Sov. Phys.–JETP* **59** 1057
[23] Ong N P and Verma G 1983 *Phys. Rev.* B **27** 4495
[24] Batistic P, Bjelis A and Gor'kov L P 1984 *J. Physique* **45** 1094
[25] Ong N P, Verma G and Maki K 1984 *Phys. Rev. Lett.* **52** 663
[26] Gill J C 1986 *J. Phys. C: Solid State Phys.* **19** 6589
[27] Borodin D V, Nad' F Ya and Zaitsev-Zotov S V 1987 *Sov. Phys.–JETP* **66** 793
[28] Csiba T, Kriza G and Janossy A 1989 *Europhys. Lett.* **9** 163